Journal of Materials Chemistry A

ROYAL SOCIETY OF CHEMISTRY

PAPER

View Article Online
View Journal | View Issue

Cite this: J. Mater. Chem. A, 2023, 11, 13552

Synthesis of ferrate (Fe(VI))-coated sand for stabilized reactivity and enhanced treatment of phenol†

Fanny E. K. Okaikue-Woodi and Jessica R. Ray *

Ferrate (Fe(VI)) is a multifunctional water treatment agent of interest due to its benign environmental impact yet effective disinfecting, coagulating, and oxidizing capabilities. Fe(VI) decomposition in water produces short-lived Fe(V) and Fe(IV) intermediates which are highly effective oxidants. Studies report that the addition of SiO_2 gels during Fe(VI) application can facilitate Fe(V) and Fe(IV) generation, and stabilize Fe(VI) reactivity for enhanced treatment. However, the application of SiO_2 gels is impractical and requires post-treatment disposal. This study leverages SiO_2 stabilization and catalytic effects on Fe(VI) reactivity to develop a Fe(VI)-coated sand water treatment media. The Fe(VI)-coated sand was synthesized by coating potassium ferrate onto sand modified with a tetraethyl orthosilicate precursor. The mass of Fe(VI) leached from the media surface increased with increasing pH (pH 7–9). Furthermore, Fe(VI) decay was faster in a borate buffer ($k = 2.22$ mg L^{-1} h^{-1}) than in a phosphate buffer ($k = 3.39$ mg L^{-1} h^{-1}). Removal of 219 ± 12 μg per L phenol—a representative wastewater organic compound—was achieved at a faster rate by the composite than by application of aqueous K_2FeO_4 powder (51% removed after 5 min compared to 37%). Decomposition of Fe(VI) from the composite surface in the presence of methyl phenyl sulfoxide (PMSO) suggests that reactive Fe(V) and Fe(IV) formation occurs at a faster rate than with K_2FeO_4 powder addition. In the presence of PMSO, phenol treatment was approximately 1.1 times higher, which suggests Fe(V)/Fe(IV) involvement. This novel, cost-effective and eco-friendly media presents a viable alternative for more feasible deployment of Fe(VI) in water treatment systems.

Received 31st March 2023
Accepted 31st May 2023

DOI: 10.1039/d3ta01950k

rsc.li/materials-a

Department of Civil & Environmental Engineering, University of Washington, 3760 E. Stevens Way, NE, Campus Box 352700, Seattle, Washington 98195-2700, USA. E-mail: jessray@uw.edu; Web: https://ray-aimslab.com/; Fax: +206-543-1543; Tel: +206-221-0791

† Electronic supplementary information (ESI) available. See DOI: https://doi.org/10.1039/d3ta01950k

Dr Jessica R. Ray (she/her) is the Robert and Irene Sylvester assistant professor in the Department of Civil & Environmental Engineering at the University of Washington. Ray also holds an adjunct appointment in the Department of Chemical Engineering. She received her BS degree in Chemical Engineering from Washington University in St. Louis in 2009. Upon graduation, Ray remained at Washington University in St. Louis to obtain a M.S. degree (2010, funded by the NSF GK-12 Graduate Research Fellowship) and a PhD in Energy, Environmental & Chemical Engineering (2015, funded by the EPA Students to Achieve Results (STAR) Fellowship). During her PhD, Ray employed surface chemistry techniques to investigate interfacial reactions of nanomaterials in water. Ray then moved to California as a Miller Institute Postdoctoral Research Fellow at the University of California, Berkeley in the Department of Civil and Environmental Engineering to develop low-cost composites to treat urban stormwater runoff. Since joining the University of Washington in 2019, Ray is continuing to develop and characterize new composite materials for selective contaminant removal in water, for enhanced degradation of persistent contaminants, and for recovery of valuable species in waste streams. In recognition of her novel, interdisciplinary research addressing urban water supply and sustainability, Chemical & Engineering News named Ray one of the "Talented 12" honorees for 2020, and in 2021 she received the NSF CAREER award.

1. Introduction

Chemical oxidation is a critical process in water treatment to facilitate the destruction of harmful trace organic compounds such as pharmaceuticals and personal care products, pesticides, antibiotics, and industrial chemicals. Traditionally, chemical oxidation is achieved by addition of ozone[1,2] or chlorine[1,3] due to their potential for disinfection. However, the application of these chemicals can lead to the formation of harmful transformation products (*e.g.*, halogenated byproducts[4–8]). For example, studies have reported increased estrogenic activity after ozonation[9,10] or chlorination[9] of estrogenic compounds (*e.g.*, bisphenol A) found in surface waters. Gomes *et al.* assessed the oxidation of a mixture of parabens—used as antimicrobial and preservatives in pharmaceuticals and personal care products—and reported quinone byproducts with higher toxicity to *D. magna*, which also demonstrates the risks associated with use of conventional chemical oxidants.[11]

Ferrate (Fe(VI)) has been explored as an alternative chemical to conventional oxidants. Fe(VI) is an environmentally benign iron oxyanion with a standard oxidation potential (E^0) of 2.2 V, which is greater than the oxidation potentials of chlorine (E^0 = 1.36 V)[12] and ozone (E^0 = 2.08 V).[12] Additionally, compared to chlorine and ozone, Fe(VI) is less reactive towards bromide[13,14] and has been shown to reduce the formation of brominated transformation byproducts during pre-oxidation of surface waters.[8,14,15] Furthermore, the chemical reduction of Fe(VI) leads to the formation of naturally occurring, non-toxic ferric (*i.e.* Fe^{3+} or Fe(III)) species[16,17] which have been used as coagulants[12,18] and adsorbents[12,19] in water treatment. Fe(VI) has been investigated in numerous studies with a demonstrated ability to remediate a wide range of organic compounds (*e.g.*, pharmaceuticals,[20–25] herbicides,[26] and other micropollutants[27–29]). The oxidation of organic compounds by Fe(VI) occurs *via*: (i) a 1 e^- transfer to form Fe(V) followed by a 2 e^- transfer to form Fe(III); (ii) a 2 e^- transfer to form Fe(II) through a Fe(IV) intermediate; (iii) reactions of Fe(V) and Fe(IV) with the compound; and (iv) an oxygen atom transfer to the compound.[30,31] Fe(VI) has high selectivity toward compounds with electron-donating moieties, but minimal reactivity toward compounds with electron-withdrawing moieties.[24] In addition, Fe(VI) has proven to be an effective coagulant[32–35] and disinfectant[35–37] in water treatment. Therefore, the large standard oxidation potential and multi-functionality of Fe(VI) make it an attractive chemical for water treatment.

While Fe(VI) is a very promising, benign treatment chemical, its deployment in water treatment applications is hindered by its aqueous properties. As the stability of the aqueous Fe(VI) chemical structure increases with solution pH, its oxidation potential decreases. Under acidic conditions, Fe(VI) exists as the short-lived and highly reactive protonated species $H_3FeO_4^+$, H_2FeO_4, and $HFeO_4^-$ (Fig. 1) which undergo hydrolysis reactions to form Fe(III) species *via* formation and decomposition of intermediate species Fe(V) and Fe(IV) phases.[38–40] Under these conditions, Fe(VI) undergoes a kinetically fast decomposition (Fig. 1A). In alkaline solutions, Fe(VI) exists as the stable and less reactive deprotonated species FeO_4^{2-} (Fig. 1) which also reacts with water to form Fe(III) *via* Fe(V) and Fe(IV) intermediate species formation.[41] Consequently, these hydrolysis reactions compete with Fe(VI)-contaminant reactions during water treatment.

In recent years, researchers have investigated methods to increase the Fe(VI) oxidizing power at environmentally relevant pH (pH 6–9).[42–48] For example, in addition to water, Fe(VI) reactions with organic compounds also generates Fe(V) and Fe(IV) intermediate species *via* one-electron and two-electron transfer respectively. Fe(V) and Fe(IV) species are reportedly two to four orders of magnitude more reactive than Fe(VI),[49] but are highly unstable and can quickly react with water to self-decompose.[29,39,40,50] Thus, enhancing reactions between the short-lived, unstable Fe(V) and Fe(IV) species and the organic compounds would improve their oxidation by Fe(VI). To this end, researchers

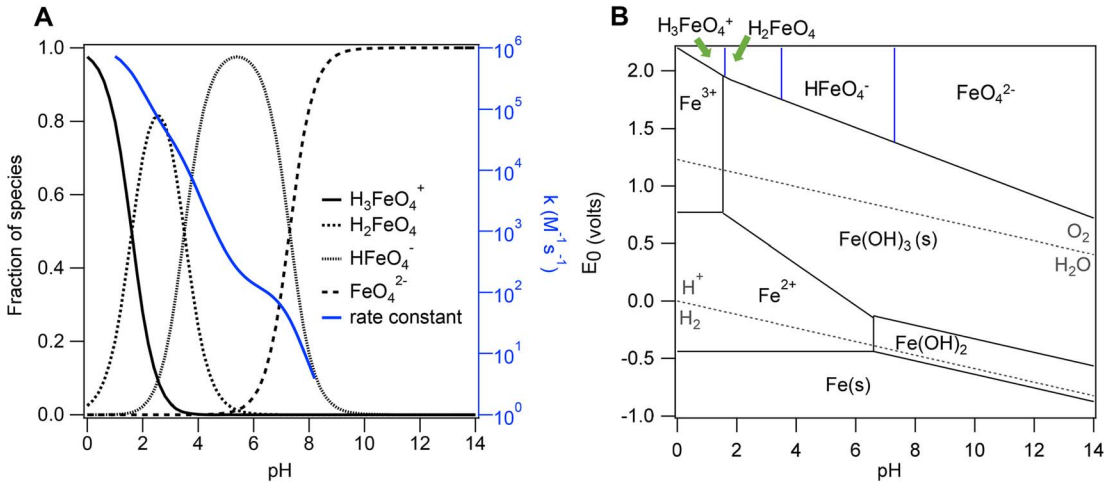

Fig. 1 (A) Speciation of Fe(VI) (left axis, black lines) and aqueous Fe(VI) self-decay rate (right axis, blue line) as a function of pH. (B) Distribution of the standard potential of iron species including Fe(VI) species. The pK_a values: $H_3FeO_4^+$ (pK_a = 1.6); H_2FeO_4 (pK_a = 3.5); $HFeO_4^-$ (pK_a = 7.3) were obtained from Rush *et al.*,[39] and decay rate constants from Lee *et al.*[50] Data for the standard potentials was obtained from Pogliani *et al.*[91] and Wulfsberg.[92]

have employed activation agents such as sulfur(IV)-based reductants[51–54] and silica (SiO_2)[30,55] to catalyze Fe(V)/Fe(IV) production. For example, Al-Abduly and Sharma reported a 22% increase in the oxidation of dibenzothiophene in the presence of SiO_2 gels at pH 8.[55] Under the same conditions (*i.e.*, pH 8, presence of SiO_2 gels), Manoli *et al.* reported a 47% increase in the oxidation of caffeine compared to oxidation in the absence of SiO_2 gels.[30] The authors proposed that interactions between Fe(VI) and SiO_2 promotes the generation of Fe(V) and Fe(IV) species, and retards the self-decomposition of Fe(VI) to Fe(V) and Fe(IV) species, thereby increasing their exposure to organic compounds.[30] During Fe(VI) oxidation of organic compounds, redox reactions between Fe(VI) and lower valence iron species (*e.g.*, Fe(II)) can occur (*e.g.*, Fe(VI) + Fe(II) → Fe(V) + Fe(III); Fe(IV) + Fe(II) → 2Fe(III))[31] which will limit Fe(VI) exposure to organic compounds and decrease Fe(VI) treatment efficacy. Studies have shown that dissolved silicate (SiO_4^{2-}) can retard the heterogeneous oxidation of Fe(II) to Fe(III) by occupying sorption sites on Fe(III) oxides.[56] Thus, the presence of SiO_2 would decrease the rate of redox reactions between iron species during Fe(VI) treatment of organic compounds.

In this study, we exploit the stabilization properties of SiO_2 to develop a novel, Fe(VI)-coated sand media for water treatment. Given the multimodal properties of Fe(VI) (*i.e.*, oxidant, disinfectant, and coagulant), researchers hypothesize that the use of Fe(VI) could reduce economical and spatial costs for water treatment plants by combining pre-disinfection, oxidation, and coagulation into one unit.[37] Therefore, the use of a Fe(VI)-coated sand media could be beneficial in water treatment systems that include filtration units as sand (composed of >80% SiO_2 content[57]) is a widely used filtration media. To assess the oxidative capacity of the novel Fe(VI)-coated sand, we will use phenol as a model organic compound as many naturally occurring and anthropogenic contaminants detected in wastewater effluents[24,58] and surface waters[24,59,60] contain phenolic moieties (*e.g.*, natural organic matter, halogenated phenols, alkylphenols, and steroid estrogens). The objectives of this study are to: (1) establish a synthesis for the Fe(VI)-coated sand media and characterize its properties; (2) assess the capacity of Fe(VI)-coated sand for the treatment of organic contaminants, and (3) elucidate the mechanisms underlying the oxidation process and the role of SiO_2 stabilization.

2. Materials and methods

2.1. Chemicals

All chemicals were ACS grade and higher unless stated otherwise. Calcium hypochlorite ($Ca(OCl)_2$), ferric nitrate nonahydrate ($Fe(NO_3)_3 \cdot 9H_2O$), and potassium hydroxide (KOH) were purchased from Fisher Scientific (Waltham, MA) and used in the synthesis of potassium ferrate (K_2FeO_4). Pentane (Sigma Aldrich, MO), methanol (JT Baker, NJ), and dichloromethane (Sigma Aldrich) were used as organic solvent washes of the K_2FeO_4 solid. The Ottawa sand composite substrate was purchased from VWR (Radnor, PA). Tetraethyl orthosilicate (TeOS, Sigma Aldrich, MO) and nitric acid (HNO_3, Fisher Scientific, MA) were used in the modification of the sand prior to Fe(VI) coating. Trace metal grade HNO_3 was purchased from Fisher Scientific for total Fe measurements. Sodium tetraborate anhydrous ($Na_2B_4O_7$, Acros Organics, Belgium), sodium phosphate dibasic heptahydrate ($Na_2HPO_4 \cdot 7H_2O$, VWR, PA), sodium phosphate monobasic monohydrate ($NaH_2PO_4 \cdot H_2O$, VWR, PA), acetic acid (Fisher Scientific, MA), sodium hydroxide (NaOH, Fisher Scientific, MA), and hydrochloric acid (HCl, Sigma Aldrich, MO) were used to prepare buffer solutions. Phenol (Sigma Aldrich, MO), methyl phenyl sulfoxide (PMSO, Sigma Aldrich, MO), methyl phenyl sulfone ($PMSO_2$, Sigma Aldrich, MO), and sodium sulfite anhydrous (Na_2SO_3, Fisher Scientific, MA) were used in the organic compound removal experiments. 2,2′-Azinobis-(3-ethylbenzothiazoline-6-sulfonate) (ABTS), 3-(2-pyridyl)-5,6-diphenyl-1,2,4-triazine-4′,4″-disulfonic acid sodium salt (ferrozine), ammonium acetate (Sigma Aldrich, MO), hydroxylamine hydrochloride (Beantown Chemical, NH), and potassium thiocyanate (KSCN, Fisher Scientific, MA) were purchased from Sigma Aldrich for measurements of aqueous Fe(VI), Fe(II), and Fe(III). High performance liquid chromatography (HPLC) grade formic acid (Agilent Technologies, CA), acetonitrile (Fisher Scientific, MA) and water (Fisher Scientific, MA) were used for HPLC analyses. All experiments were conducted using ultrapure Milli-Q water (resistivity: 18.2 mΩ).

2.2. Synthesis of Fe(VI)-coated sand

The Fe(VI)-coated sand was synthesized by adding sand to a solution of potassium ferrate. First, the Ottawa sand (30–40 mesh, >90% SiO_2) was washed with 1 M HNO_3 for 24 hours and rinsed with deionized water until the pH of the rinse solution was within pH 6–8. The washed sand was then dried at 105 °C for 24 hours in a VWR 1350G oven (Radnor, PA). To promote binding of ferrate to the sand surface, 15 mL of TeOS was added to 30 g of pre-washed sand, mixed for 3 hours, and dried at 105 °C for 24 hours in a VWR 1350G oven. The TeOS modified sand, designated as TeOS-sand, was added to the potassium ferrate (K_2FeO_4) solution. The stability of the TeOS on the sand surface was tested by sonicating 15 mg of TeOS-sand in 15 mL of 10 mM $Na_2B_4O_7$ buffer and analyzing the leachate *via* UV-vis spectroscopy using a Shimadzu UV-2700 spectrophotometer (Kyoto, Japan). The resulting spectrum was compared to the spectrum of a 4 mL TeOS solution obtained on the same spectrophotometer. Another TeOS-sand was also synthesized by mixing the TeOS (15 mL) and cleaned sand (30 g) for 24 hours before drying.

The K_2FeO_4 solution was prepared *via* the wet oxidation process following a method adapted from Guan *et al.* (more information provided in Text S1†).[61] A saturated solution of 13 M KOH was prepared, chilled, and stored at 4 °C throughout the synthesis to maintain cold temperature conditions. Approximately 15 g of $Ca(OCl)_2$ was added to 25 mL of the saturated KOH solution, then the mixture was stirred for 30–60 min and filtered using a Whatman glass microbore filter (grade GF/A) paper to obtain a yellow solution of potassium hypochlorite. An additional 20 mL of the saturated KOH solution was added to the yellow filtrate and the mixture was placed in an ice bath for 20–30 min to precipitate potassium chloride.

The potassium chloride suspension was further filtered with a GF/A filter paper, then 8 g of pulverized ferric nitrate was added in small portions (~0.50 g min^{-1}) for 15 min to the filtrate solution under cooling conditions (4 °C) to form K_2FeO_4. A VWR recirculating chiller was used to maintain the temperature of the potassium ferrate throughout the synthesis. The generated solution of potassium ferrate was stirred for an hour before the addition of 50 mL of saturated KOH. The solution was vigorously stirred at 500 rpm for 5 min and left to stand for 30 min. Next, 25 g of the TeOS-sand was added to the K_2FeO_4 solution and stirred for 24 hours at 4 °C to allow the Fe(VI) to coat the sand surface. The K_2FeO_4 supernatant was decanted, and the synthesized Fe(VI)-coated sand was centrifuged at 4000 rpm for 10 min to remove the excess solution before being dried in a VWR vacuum oven pumped with a RV12 Edwards pump for more than 24 hours. The Fe(VI)-coated sand was stored under vacuum when not in use to limit exposure to air and prevent ferrate decomposition.

2.3. Characterization of the Fe(VI)-coated sand media

2.3.1. Detection of Fe(VI) on the media surface. In an alkaline solution, Fe(VI) has an absorption peak at 510 nm.[62] The presence of the Fe(VI) on the Fe(VI)-coated sand surface was determined *via* UV-vis spectroscopy. The Fe(VI)-coated sand was placed in a 5 mM Na_2HPO_4/1 mM $Na_2B_4O_7$ solution (pH 9.25) and sonicated for 5 min to desorb Fe(VI) from the coated sand surface for direct UV-vis measurement of the Fe(VI) leachate. The leachate solution was reacted with ABTS following a method by Lee *et al.*[63] to measure the absorbance corresponding to the formation of an $ABTS^{\bullet+}$ radical at 415 nm (more information provided in Text S3†).

2.3.2. Fe coating density on the media surface. The total Fe mass coated on the sand was measured *via* inductively coupled plasma orbital emission spectrometry (ICP-OES) using a PerkinElmer Optima 8300 inductively coupled plasma-optical emission spectrophotometer (ICP-OES) (PerkinElmer, Whatman, MA) (more information provided in Text S3†). The Fe(VI)-coated sand was placed in a 1% HNO_3 solution and sonicated for 5 min to leach all the Fe coating. The leachate was further diluted with the 1% HNO_3 solution before ICP-OES analysis.

2.4. Stability of the Fe(VI) coating on the sand surface

2.4.1. Aqueous stability. Batch experiments were conducted to evaluate the aqueous stability of the Fe(VI)-coated sand and the desorption of Fe(VI) from the media surface. Approximately 50 mg of Fe(VI)-coated sand was added to 50 mL of 10 mM Na_2HPO_4/NaH_2PO_4 or 10 mM $Na_2B_4O_7$ buffer and stirred at 40 rpm. The buffer solutions were adjusted to pH 7, 8, 9 using HCl or NaOH to determine the effects of solution pH on Fe(VI) stability. At designated time intervals, aliquots of the samples were filtered using 0.2 μm, 25 mm diameter cellulose acetate syringe filters. Aqueous concentrations of Fe(VI) were determined using the ABTS method[63] and aqueous total Fe using ICP-OES (see Text S3†). Preliminary tests revealed that Fe(VI) and Fe(III) were the dominant Fe species in solution when the Fe(VI)-coated sand was placed in buffered solutions (pH 9) (Fig. S1B and C†); thus, aqueous Fe(III) concentrations were calculated as the difference between the measured total Fe and Fe(VI).

The aqueous stability of Fe(VI) in the absence of silica stabilization was also assessed for comparison with the Fe(VI)-coated sand. A stock solution of K_2FeO_4 powder (synthesis in Text S1†) was diluted to approximately 21 mg L^{-1} in 10 mM $Na_2B_4O_7$ buffer at pH 9 and stirred at 40 rpm. At designated times, a 1 mL aliquot was taken and filtered using 0.2 μm, 25 mm diameter cellulose acetate syringe filters, then residual Fe(VI) concentrations were determined using the ABTS method.[63]

2.4.2. Media storage stability. Total Fe and aqueous Fe(VI) measurements were taken at designated time intervals ($t = 1$, 3, 5, 7, and 11 days) after Fe(VI)-coated sand production to quantify Fe coating on the sand surface and to assess the media stability during storage. At each sampling time, approximately 3 g L^{-1} of Fe(VI)-coated sand was removed from the vacuum oven and placed in a 5 mM Na_2HPO_4/1 mM $Na_2B_4O_7$ solution (pH 9.25) and sonicated for 5 min to desorb Fe(VI) from the coated sand surface. The leachate solution was then reacted with ABTS to determine the aqueous Fe(VI) concentration. The same coated sand dose (3 g L^{-1}) was simultaneously measured and placed in a 1% HNO_3 solution and sonicated for 5 min before total Fe measurements.

2.5. Phenol removal experiments

Initial experiments (see Text S4†) evaluating the effect of buffering ions on the oxidation of PMSO by Fe(VI)-coated sand revealed a higher oxidation capacity of Fe(VI)-coated sand in the borate buffer thus, remaining experiments were conducted in the borate buffer. Sulfoxides (*e.g.*, dimethyl sulfoxide (DMSO), PMSO) are known to be oxidized by high-valent iron to produce their corresponding sulfones (*e.g.*, dimethyl sulfone ($DMSO_2$), $PMSO_2$) through an oxygen atom transfer step.[64] Thus, PMSO is an excellent probing compound to evaluate the media reactivity under different experimental conditions. Batch experiments to evaluate the Fe(VI)-coated sand media capacity for phenol treatment were conducted in 10 mM $Na_2B_4O_7$ buffer at pH 9 in media bottles wrapped with aluminum foil to maintain dark conditions.

The effect of Fe(VI)-coated sand dose on phenol removal was determined to identify the optimal media dose for water treatment. Different amounts (*i.e.*, 22.8 ± 1.1, 42.6 ± 0.8, and 80.7 ± 1.0 mg) of Fe(VI)-coated sand were added to 20 mL solutions of 10 mM $Na_2B_4O_7$ containing phenol (236 ± 0.6 μg L^{-1}) to obtain media doses of 1, 2, and 4 g L^{-1}. The mixtures were shaken for 30 min at 40 rpm. Then, a 2 mL aliquot was quenched with 20 μL of 500 mM Na_2SO_3 to stop the reaction between Fe(VI) and phenol. The mixture was filtered with a 0.2 μm, 25 mm diameter cellulose acetate syringe filter to measure residual phenol using high performance liquid chromatography (HPLC) methods. Details of the HPLC method are provided in Text S4.†

Removal kinetics experiments were initiated by adding approximately 200 mg of Fe(VI)-coated sand to 100 mL of a 10 mM $Na_2B_4O_7$ buffer solution containing phenol. At designated time intervals, an aliquot of 2 mL was sampled and pretreated as above before HPLC analysis. An additional aliquot of

1 mL was taken simultaneously to measure aqueous Fe(VI) concentration by the ABTS method.[63] Another 1 mL aliquot was further diluted with a 10 mM $Na_2B_4O_7$ buffer solution and quenched with HNO_3 (trace metals grade) to measure total aqueous Fe by ICP-OES. A 4 mL aliquot was also taken and filtered with a 0.2 μm, 25 mm diameter cellulose acetate syringe filter for UV-vis scanning between 200 and 650 nm for detection of oxidation products with absorbances outside of the range of the HPLC diode array detector.

The removal of phenol by Fe(VI) powder was also investigated to compare the performance of the Fe(VI)-coated sand media against Fe(VI) powder in the absence of silica stabilization. Fe(VI) stock solution (*i.e.*, in the absence of sand) was freshly prepared by diluting approximately 12.6 mg L^{-1} of K_2FeO_4 powder (synthesis details in Text S1†) in 10 mM $Na_2B_4O_7$ buffer. The stock solution was used within 15 min of preparation to minimize Fe(VI) self-decay. 10 mL of the stock solution was added to 90 mL of a 10 mM $Na_2B_4O_7$ buffer solution containing phenol to initiate phenol removal. All experiments were conducted in duplicates or triplicates.

2.6. Evaluation of Fe(VI)-coated sand oxidation mechanisms

To assess the media reactivity toward multiple organic compounds and probe oxidation mechanisms, phenol removal by Fe(VI)-coated sand was assessed in the presence of PMSO. Fe(VI)-coated sand (2 g L^{-1}) was added to pH 9 borate buffer solutions containing PMSO and phenol at different concentrations (250 or 500 μg per L phenol and 400 μg per L or 800 μg per L PMSO). Aliquots were sampled and analyzed as described in Section 2.5. HPLC samples were analyzed for phenol, PMSO and $PMSO_2$. All experiments were conducted in duplicates or triplicates.

3. Results and discussion

3.1. TeOS sand surface modification increases Fe(VI) coating density

Spectroscopic characterization of modified sand surfaces indicates greater Fe(VI) coating densities in the presence of TeOS. The Fe(VI)-coated sand synthesis method proposed in this study generates a purple-grey sand product (Fig. 2A) which appears dark purple when placed in aqueous solution (Fig. 2B). The purple color is indicative of the Fe(VI) speciation.[65] UV-vis measurements confirmed the presence of Fe(VI) on the sand surface (Fig. S1A†). Direct measurements of the leachate after the Fe(VI)-coated sand was added to a phosphate/borate buffer (5 mM Na_2HPO_4/1 mM Na_2B4O_7) solution shows a maximum absorbance at 509 nm (Fig. S1A†) confirming the presence of Fe(VI) on the coated sand surface.[62] Furthermore, the reaction between the leachate and ABTS generated the expected $ABTS^{\bullet+}$ radical[63] as evidenced by the absorbance peak at 415 nm (Fig. S1A†). Fe(VI) reacts rapidly with ABTS *via* a one-electron transfer mechanism to produce the stable radical $ABTS^{\bullet+}$. The $ABTS^{\bullet+}$ absorbance at 415 nm is then used to calculate aqueous Fe(VI) concentration.

TeOS modification of the sand prior to Fe(VI) coating increased Fe(VI) binding to the sand surface (Fig. 2D). TeOS is a well-known silica precursor[66,67] that has been used to stabilize iron oxide particles.[68] ICP-OES analysis of the temporal Fe leached from the Fe(VI)-coated sand revealed that Fe(VI)-coated sand synthesized with TeOS-sand had approximately 44% higher initial Fe loading (Fig. 2D) than media prepared with unmodified sand, indicating a higher Fe coating density in the presence of TeOS. Furthermore, ICP-OES analysis of acid-treated leachate—which revealed the maximum Fe loading on the sand surfaces—from the TeOS modified and unmodified sand surfaces (Fig. S2†) confirm that TeOS modification increases Fe coating mass. Additionally, spectroscopic analysis revealed a stable TeOS coating (*i.e.*, no leaching of TeOS) on the sand surface (Fig. S3†). The UV-vis spectrum of the supernatant of TeOS-sand sonicated in the 10 mM borate buffer did not show an absorbance peak at 292 nm as corresponding to the presence of TeOS (Fig. S3†).

3.2. Solution pH and buffering ions govern Fe(VI)-coated sand stability

Analysis of Fe(VI) leaching kinetics suggests that the media Fe(VI) aqueous stability increases with increasing pH. Leaching

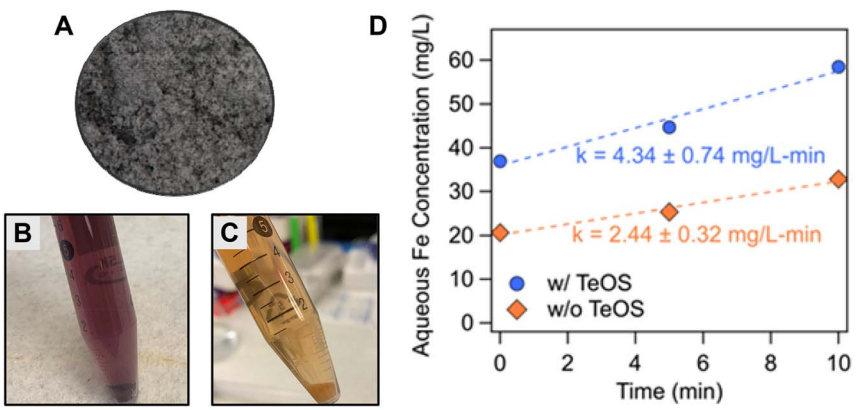

Fig. 2 (A) As-prepared Fe(VI)-coated sand with TeOS-sand modification. (B) 20 g per L Fe(VI)-coated sand added to 5 mM Na_2HPO_4/1 mM NaB_4O_7 solution at time $t = 0$ and (C) at $t = 180$ min indicating Fe(VI) (purple) reduction to Fe(III) (orange) phases. (D) Total Fe leached from the Fe(VI)-coated sand prepared with and without TeOS-sand modification (3 h reaction).

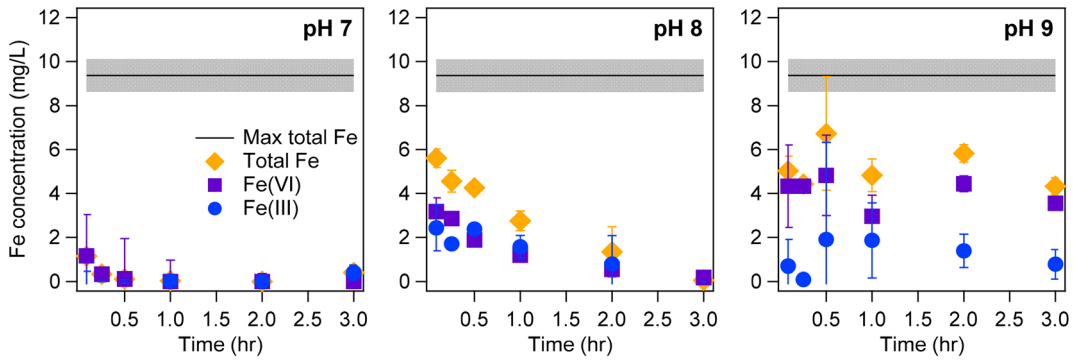

Fig. 3 Kinetics of Fe(VI), Fe(III) and total Fe leached from 1 g per L Fe(VI)-coated sand into a 10 mM $Na_2B_4O_7$ solution at pH 7, 8, 9 as a function of time. Max total Fe refers to the maximum mass of Fe that would leach of the surface of Fe(VI)-coated sand. This was determined by mixing 1 g per L Fe(VI)-coated sand into 1% HNO_3 and measuring total Fe in solution. Total Fe refers to the total Fe leached into solution at a given time.

experiments were conducted with the Fe(VI)-coated sand in buffered solutions (10 mM phosphate and 10 mM borate) at pH 7, 8, and 9 to evaluate the effect of pH and inorganic ions on the aqueous stability of the media (Fig. 3, S4 and S5†). Initially, the Fe(VI)-coated sand was sonicated in 1% HNO_3 to desorb all the Fe from the coated sand surface and to quantify the total Fe coating density on the media. This total Fe (9.4 ± 0.8 mg L^{-1}) is designated as the maximum total Fe coating on the sand. The maximum total Fe concentration was greater than the aqueous total Fe concentrations at time t ($t = 5$–180 min) suggesting that Fe(VI) desorption from the coated sand is not instantaneous (Fig. 3 and S5†). Previous studies have proposed that organic contaminant oxidation can be improved by a slow release of Fe(VI) into solution during water treatment[69–71] or multi-step dosing of Fe(VI).[25,72] These two application methods limit Fe(VI) self-decay and increase Fe(VI) exposure to organic contaminants.[29] Similarly, a delayed desorption of Fe(VI) from the coated sand surface presents an opportunity for improved treatment of organic contaminants during water treatment. In solution, the Fe(VI)-coated sand media would consist of: (i) aqueous Fe(VI) leached from the sand surface; (ii) aqueous Fe(III) leached from the sand surface or produced from aqueous Fe(VI) decay; (iii) Fe(III) solids suspended in solution; and, (iv) Fe(VI) and/or Fe(III) bound to the sand surface. Thus, contaminant removal can occur simultaneously *via* reactions with Fe(VI) and Fe(III) in different phases and configurations. Further investigations on the coated sand surface and the Fe(III) phases produced are needed to differentiate these phases and elucidate mechanisms by which contaminants are removed on the Fe(VI)-coated sand surface.

The Fe(VI)-coated sand exhibited slower decomposition kinetics at circumneutral pH. Previous studies reported that Fe(VI) was the most stable in aqueous solutions buffered at pH 9.2–9.4, but experienced a kinetically fast decay below this pH range.[73] Our Fe(VI) stability tests also confirm that the Fe(VI) leached from the Fe(VI)-coated sand was more stable at pH 9 than at pH 7 and 8. Aqueous decomposition of Fe(VI) was minimal at pH 9 (Fig. 3 and S5†). The aqueous Fe(VI) decay rates in the borate buffer were estimated at 355.4, 0.82, 0.004 mg^{-1} L^{-1} h^{-1} at pH 7, 8, 9 respectively (Fig. S6†). At pH 7, the dominant Fe(VI) species is $HFeO_4^-$ (~67%) (Fig. 1) which has a higher oxidizing potential[74,75] than the deprotonated FeO_4^{2-}. The high oxidizing potential of the dominant $HFeO_4^-$ species and fast reactions with water result in the instability of aqueous Fe(VI) at pH 7 (Fig. 3, S4 and S5†). The self-decay of aqueous Fe(VI) was lessened at pH 8 (Fig. 3 and S5†) and can be attributed to the dominant species, FeO_4^{2-} (~83%) (Fig. 1) being less reactive than the $HFeO_4^-$ species.[74] Due to the increased production of Fe(III) at pH 7 and 8, we hypothesize that sorption and coagulation are the major mechanism of contaminant removal whereas at pH 9, oxidation of organic compounds may be the more dominant treatment mechanism. At pH values where Fe(VI) decays faster, the treatment of organic contaminants by the Fe(VI)-coated sand media may occur by these pathways: (i) physical adsorption of the contaminants on the coated sand surface followed by oxidation by surface-bound Fe(VI) species; (ii) sorption to surface-bound Fe(III) particles; (iii) limited oxidation by Fe(VI) in the aqueous phase; and, (iv) sorption and coagulation with Fe(III) particles in the aqueous phase. Characterization of optimized Fe(VI) stability is important in determining the operating conditions of Fe(VI)-coated sand application for which contaminant treatment is maximized, and will be explored in future studies.

The aqueous stability of the Fe(VI)-coated sand is also affected by the buffering ions (Fig. 3, S4 and S5†). At pH 8 and 9, aqueous Fe(VI) and total aqueous Fe concentrations were lower in the borate buffer than in the phosphate buffer (Fig. 3 and S5†). At pH 8, the total aqueous Fe concentration in the borate buffer within 0.5 hour of mixing was 4.26 ± 0.27 mg L^{-1} and 7.43 ± 0.76 mg L^{-1} in the phosphate buffer. Additionally, we noted that total Fe concentrations at pH 7 and 8 were constant in the phosphate buffer (Fig. S5†), yet the Fe concentration decreased with time in the borate buffer except at pH 9 (Fig. 3). These results imply that while Fe desorption from the media surface is lessened in the borate buffer, Fe(VI) decay was enhanced. A linear regression fitted to the measured Fe(VI) concentrations in both buffered solutions at pH 8 shows that the slope for the borate buffer was 65% smaller than the slope for the phosphate buffer (Fig. S7†) indicating that Fe(VI) decay was slower in the phosphate buffer. This result is in agreement

with previous studies where Fe(VI) self-decay at pH 7.5 was slower in a 10 mM phosphate buffer than in a 10 mM borate buffer.[76] The results of the leaching experiments suggest faster Fe(VI) decay would occur when the Fe(VI)-coated sand media is placed in certain pH and buffering conditions. In particular, water chemistries that favor the presence of Fe(III) would promote rapid decay of Fe(III) due the catalytic effect of Fe(III) species on Fe(VI) self-decay.[76,77] The presence of Fe(III) in solution will result in a decrease in solution pH,[78] thus increasing the Fe(VI) oxidizing potential (*via* formation of protonated Fe(VI) species and reactive intermediate species) and promoting reactions with water molecules which would catalyze further decay of Fe(VI).[79] However, phosphate ions can form metal complexes with Fe(III) and prevent the formation of iron colloids and solids,[76,80] thus impeding the Fe(III) catalytic effect on Fe(VI) decay. This complexation behavior can explain the reduced Fe(VI) decay observed in the phosphate buffer in this study (Fig. S7†). In the absence of phosphate ions, Fe(III) particles aggregate to form larger particles.[76,80] Thus, the temporal decrease in total Fe observed at pH 7 and 8 in the borate buffer (Fig. 3) can be attributed to these larger particles being removed by filtration which was done prior to ICP-OES analysis of the samples.

Further stability tests indicate that the proposed synthesis method generates a stable and viable media. We assessed the stability of Fe(VI) when K_2FeO_4 powder is dissolved in the borate buffer at pH 9 (Fig. S8†). Results revealed that in this system, Fe(VI) decay faster at a rate of 1.14 mg L^{-1} h^{-1} compared to the Fe(VI)-coated sand where Fe(VI) decay was estimated at 0.23 mg L^{-1} h^{-1}. This result validates the SiO_2 stabilization effect on Fe(VI). Additionally, the stability of the stored media was assessed by determining changes in total Fe and Fe(VI) on the sand surface at time *t* (in days) after the media was produced (Fig. S9†). The total measured Fe varied between 5.69 ± 0.99 to 7.39 ± 1.01 mg Fe per g sand. The degree of variability could be due to slight differences in coating density at different sites on the sand surface. Fe(VI) concentrations (~2.43 mg Fe(VI) per g sand) remained constant for up to 7 days after media production then slightly decreased (1.29 mg Fe(VI) per g sand) after 7 days.

3.3. Silica-stabilized Fe(VI) improves the treatment of phenol

While phosphate ions reduces Fe(VI) self-decay, studies have reported that their presence in solution leads to decreased oxidation of organic compounds by Fe(VI).[81] Huang *et al.* observed removal efficiencies of 97%, 90%, and 95% of carbamazepine, diclofenac, and ciprofloxacin, respectively, in unbuffered river waters but only 85%, 74%, and 82% removal of these compounds in phosphate buffered river waters.[81] The oxidation of organic compounds by Fe(VI) occur *via* (i) reactions between Fe(VI) and the compounds to form Fe(V) or Fe(IV), which are more reactive than Fe(VI); and, (ii) further reactions between the compounds and Fe(IV)/Fe(V).[30,31] However, phosphate ions can react with Fe(V) through a nucleophilic attack to form metal complexes which would lead to a decrease in Fe(V) reactivity and thus reduce the oxidation of organic compounds.[81] On the other hand, borate ions have lower reactivity towards Fe species.[50,76,82] Our observations on the oxidation of PMSO by Fe(VI)-coated sand in 10 mM phosphate and borate buffer corroborated these findings (Fig. S10†). The oxidation efficiency of PMSO in the borate buffer was 93% (Fig. S10B†) but only 26% (Fig. S10A†) in the phosphate buffer under the same experimental conditions (*i.e.*, pH 9, 2 g per L Fe(VI)-coated sand and 1 hour reaction time). The lower concentration of $PMSO_2$ observed in the phosphate buffer reaction system confirms the negative effect of phosphate ions on Fe(VI) reactivities (Fig. S10†).

Phenol removal increased with increasing doses of the Fe(VI)-coated sand. The Fe(VI)-coated sand dose used in this study was determined by assessing the effect of different media doses (*i.e.*, 1, 2 and 4 g L^{-1}) on the removal of phenol. Our results indicate that removal of phenol improved with increasing media doses and plateaued after 2 g L^{-1} (Fig. 4). At this dose, 97% removal of phenol at an initial concentration of 236 μg L^{-1} was achieved. Thus, a dose of 2 g L^{-1} was chosen for further experiments.

Coating Fe(VI) onto the sand substate enhances its treatment capability toward organic compounds. The removal of phenol by the Fe(VI)-coated sand was compared to removal by the as-prepared K_2FeO_4 powder application (Fig. 5 and S11†). Both media had similar removal efficiencies (85% for as-prepared K_2FeO_4 powder and 83% for Fe(VI)-coated sand) of phenol at

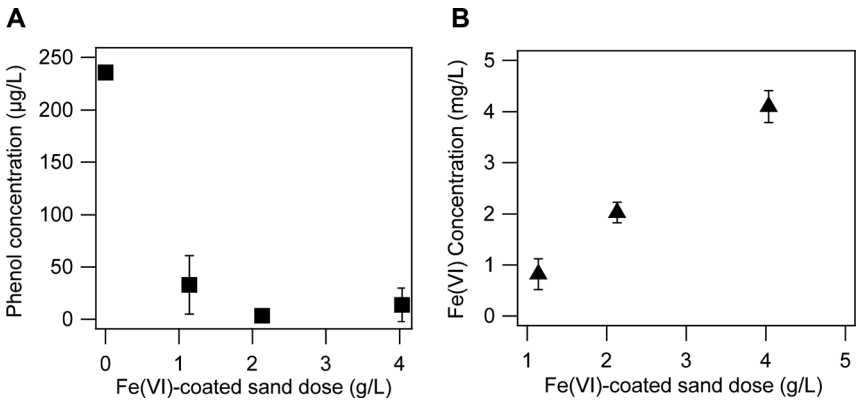

Fig. 4 (A) Effect of Fe(VI)-coated sand dose on the removal of 236 ± 0.6 μg per L phenol in 10 mM borate buffer pH 9 and (B) the measured Fe(VI) concentration remaining in solution after 30 min of reaction with phenol treatment.

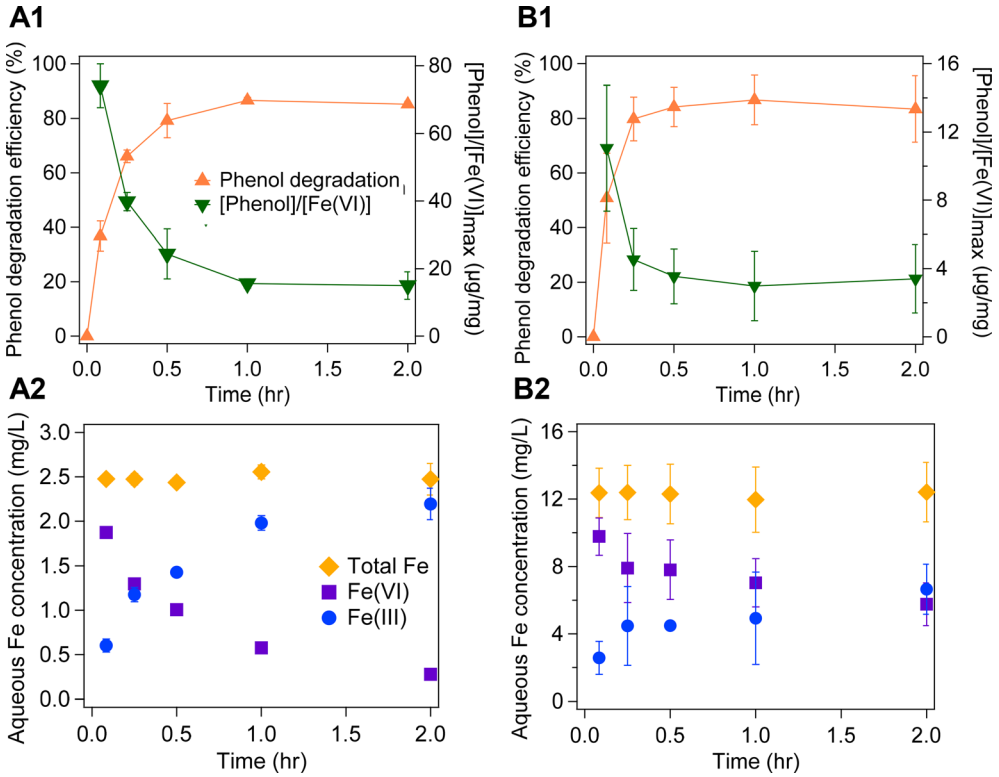

Fig. 5 Degradation of 219 ± 12 μg per L phenol in 10 mM borate buffer pH 9 by (A) 12.6 mg per L Fe(VI) powder and (B) 2 g per L Fe(VI)-coated sand. (Top) phenol removal efficiency (left axis) and phenol to maximum aqueous Fe(VI) concentrations ratio (right axis) with time; Fe(VI) concentration at 5 min was taken as the maximum aqueous Fe(VI) concentration, (bottom) changes in aqueous Fe.

the end of the 2 h reaction time; however, phenol removal was faster by the Fe(VI)-coated sand (Fig. 5 and S11†). After 5 min, the removal of phenol by Fe(VI)-coated sand was 51%, but only 37% by the as-prepared K_2FeO_4 powder. This accelerated treatment by Fe(VI)-coated sand could lead to rapid degradation of organic contaminants which has economic benefits for water treatment plants. Under the experimental conditions of this study (*i.e.*, 2 g per L Fe(VI)-coated sand and 12.6 mg L^{-1} as-prepared K_2FeO_4 powder), we observed higher aqueous Fe(VI) concentrations (5.76–9.77 mg L^{-1}) in the Fe(VI)-coated sand system than in the as-prepared K_2FeO_4 powder (0.28–1.87 mg L^{-1}), which could explain the enhanced treatment of phenol by Fe(VI)-coated sand. Previous studies have reported increased oxidation of organic compounds as Fe(VI) doses increase.[30,83] However, we observed a faster decay of aqueous Fe(VI) in the as-prepared K_2FeO_4 powder system compared to the Fe(VI)-coated sand system (Fig. 5A2–B2). We hypothesize that the slower decay of Fe(VI) in the Fe(VI)-coated sand system indicates more Fe(VI) available in solution for longer periods of time, which also suggests that more organic compounds could be treated simultaneously by the Fe(VI)-coated sand. The slower Fe(VI) decay in the Fe(VI)-coated sand system also confirms the SiO_2 stabilization effect on Fe(VI) reactivity. Furthermore, reduced decay rates of aqueous Fe(VI) also generate lower quantities of Fe(III) particles in solution which could decrease the frequency for Fe(III) sludge disposal post-treatment. Based on our hypothesis in Section 3.2, we speculate that phenol removal by Fe(VI)-coated sand would be threefold: removal or degradation in the aqueous phase, sorption/coagulation with Fe(III) solids, and removal or degradation on the sand surface. Further investigations are needed to characterize and decouple these removal mechanisms. For example, Huang *et al.* reported that the oxidation of phenol by Fe(VI) leads to the formation of a quinone and biphenol products *via* a phenoxy radical.[84]

UV-vis measurements from reactions of phenol and Fe(VI)-coated also indicate the potential formation of oxidation products (Fig. S12†). We observed a sharp peak at 307 nm, a small shoulder peak near 350 nm, and a broad peak in the range of 430–630 nm with maximum absorbance near 500 nm (Fig. S12†). These peaks were not seen in the spectrum of a phenol control solution (*i.e.*, no Fe(VI), Fig. S12†). We suspect that the broad peak around 500 nm could be attributed to Fe(VI) which has an absorbance at 509 nm (Fig. S1A†) rather than an oxidation product. The minimal change in the absorbance values at this peak (Fig. S12†) aligns with the stable aqueous Fe(VI) concentration observed during phenol treatment by Fe(VI)-coated sand (Fig. 5B2). The absorbance peak at 307 nm may be attributed to an oxidation product. The continuous increase in absorbance values at this peak indicates increased formation of the oxidation product as phenol degradation progresses (Fig. 6 and S12†). Chen *et al.* reported the oxidation of phenol *via* hydroxylation of the benzene ring which forms a hydroquinone intermediate product that further converts into *p*-benzoquinone and other oxidation products.[85] UV-vis measurement of

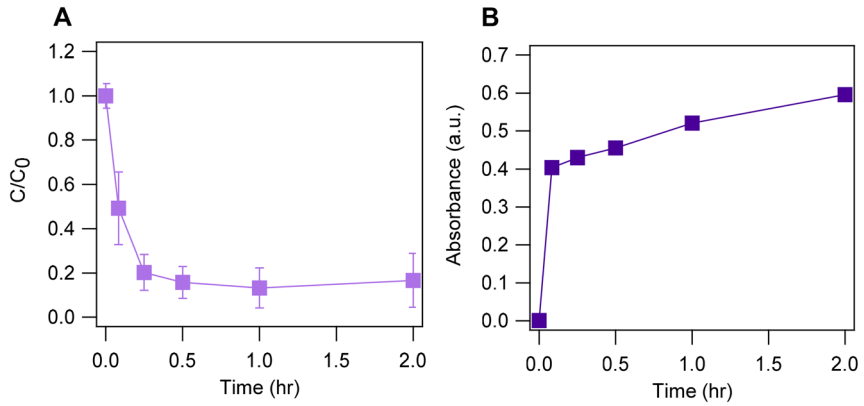

Fig. 6 (A) Degradation of 219 ± 12 μg per L phenol by 2 g per L Fe(VI)-coated sand in 10 mM borate buffer pH 9 and (B) subsequent formation of the oxidation product with maximum absorbance at 307 nm.

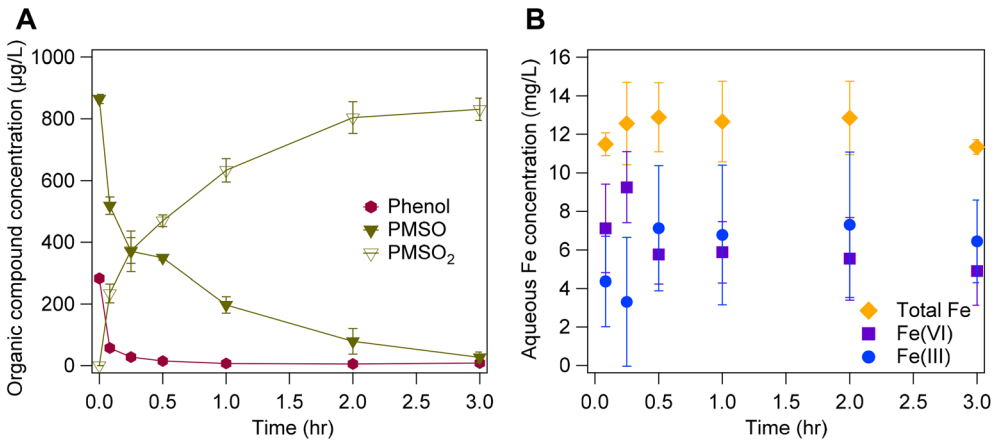

Fig. 7 (A) Removal of 283 ± 2.1 μg per L phenol and 865 ± 15 μg per L PMSO by 2 g per L Fe(VI)-coated sand. (B) Changes in aqueous Fe concentration.

hydroquinone in 10 mM borate buffer showed absorbance peaks at 290, 316, 403 and 428 nm (Fig. S12†). Previous studies have reported an absorbance peak at 293 nm (ref. 86) and 289 nm (ref. 87) for hydroquinone. We speculate that the oxidation product formed in this study may be a quinone product. However, further analyses and more targeted analytical tools (*e.g.*, mass spectrometry, gas chromatography) will be performed to monitor and identify all oxidation products formed.

Fe(VI)-coated sand had greater reactivity towards phenol in the presence of PMSO (Fig. 7 and S13†) which indicates an increased presence of reactive species. The removal capacity of Fe(VI)-coated sand for phenol and PMSO was assessed using different concentrations of the organic compounds (*i.e.*, 283 μg per L phenol and 865 μg per L PMSO; 245 μg per L phenol and 394 μg per L PMSO; and, 520 μg per L phenol and 739 μg per L PMSO). In the absence of PMSO, phenol removal by Fe(VI)-coated sand was estimated at 51% within 5 min (Fig. 5), whereas in the presence of PMSO, the removal efficiency was 80–97% (Fig. 7 and S13†). The increased removal of phenol in the presence of PMSO suggests the formation of other reactive species (*i.e.*, Fe(V), Fe(IV)), as a result of the reaction between Fe(VI)-coated sand and PMSO.[88] The complete oxidation of PMSO to $PMSO_2$ (Fig. 7) in this study indicates the presence of Fe(V) and Fe(IV) species and no other reactive species (*i.e.*, H_2O_2) which would oxidize PMSO into other products.[64] Consequently, Fe(V) and Fe(IV) yield will increase due to their production from Fe(VI) self-decay and Fe(VI) reaction with PMSO thereby increasing phenol removal. These results also corroborate previous hypotheses[30,48] regarding the SiO_2 stabilization effects on the rapid formation of Fe(V) and Fe(IV) in Fe(VI) systems. Thus, in multi-pollutants systems, the combination of greater Fe(VI) reactivity promoted by SiO_2 and Fe(V)/Fe(IV) production from Fe(VI) reactions could result in more effective treatment than in aqueous K_2FeO_4 powder systems.

4. Conclusion

This study demonstrates a novel Fe(VI)-coated sand water treatment media application for organic contaminant removal. A synthesis method is proposed to produce a viable and stable Fe(VI)-coated sand composite. The initial coating of the sand with tetraethyl orthosilicate yielded a Fe(VI)-coated sand media with higher Fe (44%) bound to the surface and a greater binding

attachment than media produced without sand modification. Water chemistries (*i.e.*, pH and buffers) were explored to determine their effect on the rate of Fe(VI) decomposition and leaching from the media surface. The Fe(VI) self-decay was accelerated at pH 7 ($k = 3.87$ mg^{-1} L^{-1} h^{-1}) and slowed with increasing pH ($k = 0.04$ mg^{-1} L^{-1} h^{-1} at pH 9). Borate ions promoted a faster decay ($k = 2.22$ mg L^{-1} h^{-1}) of the media compared to phosphate ions ($k = 3.39$ mg L^{-1} h^{-1}). Treatment of phenol by the Fe(VI)-coated sand and by K_2FeO_4 powder revealed that the composite media had a removal capacity that is 1.4 times greater than that of Fe(VI) powder. Furthermore, the fast and complete removal of phenol (with initial concentrations of 245–283 μg L^{-1}) in the presence of PMSO (with initial concentrations of 394–865 μg L^{-1}) compared to the incomplete removal of phenol in the absence of PMSO indicates an increased production of highly reactive Fe(V) and Fe(IV) intermediate species.

Removal of organic compounds by the media is expected to be three-fold: removal or oxidation by aqueous Fe(VI), adsorption by suspended Fe(III) particles, and removal or oxidation on sand surface. Further testing is needed to distinguish these different mechanisms, identify the oxidation products and pathways, and better understand the Fe(VI)-coated sand functionality.

Coating Fe(VI) onto a sand surface presents an opportunity for increasing Fe(VI) stability and for better deployment of Fe(VI) in water treatment applications. Previous studies have reported advantages of heterogeneous Fe(VI) applications.[46,89,90] This study offers an environmentally benign media that would be applicable to treatment systems (*e.g.*, advanced wastewater systems) where sand filtration systems are already in use. Our Fe(VI)-coated sand media limits the need for solid substrates like SiO_2 gels that may require post-treatment disposal. The reduction of Fe(VI) to Fe(III) after treatment and the potential for synergistic treatment processes (*i.e.*, oxidation, coagulation, disinfection, and filtration) due to Fe(VI) multimodal properties make this novel Fe(VI)-coated sand a cost-effective and eco-friendly water treatment media suitable for deployment in many water treatment applications. Currently, there are commercialized processes in place for on-site Fe(VI) production at water treatment facilities, which eliminates transportation costs. These cheaper Fe(VI) production methods coupled with the inexpensive cost of sand ($33 per kg) and TeOS ($64 per L) make the Fe(VI)-coated sand synthesis a cost-effective process.

Conflicts of interest

The authors declare that they have no known competing financial interests or personal relationships that could have appeared to influence the work reported in this paper.

Acknowledgements

This research was supported by the Washington Research Foundation. We are grateful to Joseph Severin, Megan Vance, and Michelle Kane for the assistance in obtaining data (*e.g.*, Fe(VI)-coated sand synthesis, UV-vis measurements, data analysis) for this work. We would like to thank Yiran Wan from Sichuan University who was supported by the Hong Kong Polytechnic University Institute for Disaster Management and Reconstruction Innovation Class Program for assistance with kinetic experiments of phenol and K_2FeO_4 powder. We would also like to thank Dr Michael C. Dodd for use of the VWR recirculating chiller needed for Fe(VI) synthesis. We would like to thank Dr Adrienne Roehrich at the Spectroscopic and Analytical Instrumentation Facility in the Department of Chemistry at the University of Washington for support during use of the ICP-OES. Part of this work was conducted at the Washington Clean Energy Testbeds, a facility operated by the University of Washington Clean Energy Institute. We would like to thank Dr Philip Cox for assistance with the vacuum oven used during synthesis of the Fe(VI)-coated sand. We would also like to thank the Washington Research Foundation and University of Washington Royalty Research Fund for funding a portion of this work.

References

1 U. Von Gunten, *Environ. Sci. Technol.*, 2018, **52**, 5062–5075.
2 U. Von Gunten, *Water Res.*, 2003, **37**, 1443–1467.
3 J. Wenk, M. Aeschbacher, E. Salhi, S. Canonica, U. Von Gunten and M. Sander, *Environ. Sci. Technol.*, 2013, **47**, 11147–11156.
4 U. Von Gunten, *Water Res.*, 2003, **37**, 1469–1487.
5 Y. Pan and X. Zhang, *Environ. Sci. Technol.*, 2013, **47**, 1265–1273.
6 D. B. Miklos, C. Remy, M. Jekel, K. G. Linden, J. E. Drewes and U. Hubner, *Water Res.*, 2018, **139**, 118–131.
7 E. Rodríguez, G. D. Onstad, T. P. J. Kull, J. S. Metcalf, J. L. Acero and U. Von Gunten, *Water Res.*, 2007, **41**, 3381–3393.
8 Q. Han, H. Wang, W. Dong, T. Liu and Y. Yin, *Sep. Purif. Technol.*, 2013, **118**, 653–658.
9 J.-Y. Hu, T. Aizawa and S. Ookubo, *Environ. Sci. Technol.*, 2002, **36**, 1980–1987.
10 A. Alum, Y. Yoon, P. Westerhoff and M. Abbaszadegan, *Environ. Toxicol.*, 2004, **19**, 257–264.
11 J. F. Gomes, D. Frasson, J. L. Pereira, F. J. M. Goncalves, L. M. Castro, R. M. Quinta-Ferreira and R. C. Martins, *Chem. Eng. J.*, 2019, **360**, 30–37.
12 J.-Q. Jiang and B. Lloyd, *Water Res.*, 2002, **36**, 1397–1408.
13 V. K. Sharma, *J. Environ. Manage.*, 2011, **92**, 1051–1073.
14 Y. Jiang, J. E. Goodwill, J. E. Tobiason and D. A. Reckhow, *Water Res.*, 2016, **96**, 188–197.
15 J. Liu, H. Lujan, B. Dhungana, W. C. Hockaday, C. M. Sayes, G. P. Cobb and V. K. Sharma, *Environ. Int.*, 2020, **138**, 105641.
16 R. H. Wood, *J. Am. Chem. Soc.*, 1958, **80**, 2038–2041.
17 V. K. Sharma, *Adv. Environ. Res.*, 2002, **6**, 143–156.
18 J.-Q. Jiang, S. Wang and A. Panagoulopoulos, *Chemosphere*, 2006, **63**, 212–219.
19 L. Hao, M. Liu, N. Wang and G. Li, *RSC Adv.*, 2018, **8**, 39545–39560.
20 C. Li, X. Z. Li, N. Graham and N. Y. Gao, *Water Res.*, 2008, **42**, 109–120.

21 V. K. Sharma, S. K. Mishra and N. Nesnas, *Environ. Sci. Technol.*, 2006, **40**, 7222–7227.
22 V. K. Sharma, S. K. Mishra and A. K. Ray, *Chemosphere*, 2006, **62**, 128–134.
23 G. A. K. Anquandah, V. K. Sharma, D. A. Knight, S. R. Batchu and P. R. Gardinali, *Environ. Sci. Technol.*, 2011, **45**, 10575–10581.
24 B. Yang, G.-G. Ying, J.-L. Zhao, S. Liu, L.-J. Zhou and F. Chen, *Water Res.*, 2012, **46**, 2194–2204.
25 M. Feng, X. Wang, J. Chen, R. Qu, Y. Sui, L. Cizmas, Z. Wang and V. K. Sharma, *Water Res.*, 2016, **103**, 48–57.
26 P. Zajíček, M. Kolář, R. Prucek, V. Ranc, P. Bednář, R. S. Varma, V. K. Sharma and R. Zbořil, *Sep. Purif. Technol.*, 2015, **156**, 1041–1046.
27 Y. Lee, S. G. Zimmermann, A. T. Kieu and U. Von Gunten, *Environ. Sci. Technol.*, 2009, **43**, 3831–3838.
28 V. K. Sharma, L. Chen and R. Zboril, *ACS Sustainable Chem. Eng.*, 2016, **4**, 18–34.
29 S. Wang, B. Shao, J. Qiao and X. Guan, *Front. Environ. Sci. Eng.*, 2021, **15**, 80.
30 K. Manoli, G. Nakhla, M. Feng, V. K. Sharma and A. K. Ray, *Chem. Eng. J.*, 2017, **330**, 987–994.
31 V. K. Sharma, R. Zboril and R. S. Varma, *Acc. Chem. Res.*, 2015, **48**, 182–191.
32 R. Prucek, J. Tucek, J. Kolarik, I. Huskova, J. Filip, R. S. Varma, V. K. Sharma and R. Zboril, *Environ. Sci. Technol.*, 2015, **49**, 2319–2327.
33 M. Lim and M.-J. Kim, *Water Air Soil Pollut.*, 2010, **211**, 313–322.
34 J. E. Goodwill, X. Mai, Y. Jiang, D. A. Reckhow and J. E. Tobiason, *Chemosphere*, 2016, **159**, 457–464.
35 J. Cui, L. Zheng and Y. Deng, *Environ. Sci. Water Res. Technol.*, 2018, **4**, 359–368.
36 J. Fan, B.-H. Lin, C.-W. Chang, Y. Zhang and T.-F. Lin, *Water Res.*, 2018, **129**, 199–207.
37 J. Q. Jiang, S. Wang and A. Panagoulopoulos, *Chemosphere*, 2006, **63**, 212–219.
38 G. Chen, W. W. Y. Lam, P. K. Lo, W. L. Man, L. Chen, K. C. Lau and T. C. Lau, *Chem.–Eur. J.*, 2018, **24**, 18735–18742.
39 J. D. Rush, Z. Zhao and B. H. J. Bielski, *Free Radical Res.*, 1996, **24**, 187–198.
40 R. Sarma, A. M. Angeles-Boza, D. W. Brinkley and J. P. Roth, *J. Am. Chem. Soc.*, 2012, **134**, 15371–15386.
41 C. Luo, M. Feng, V. K. Sharma and C.-H. Huang, *Chem. Eng. J.*, 2020, **388**, 124134.
42 M. Feng, L. Cizmas, Z. Wang and V. K. Sharma, *Chem. Eng. J.*, 2017, **323**, 584–591.
43 M. B. Feng, L. Cizmas, Z. Y. Wang and V. K. Sharma, *Chemosphere*, 2017, **177**, 144–148.
44 K. Manoli, R. Li, J. Kim, M. Feng, C.-H. Huang and V. K. Sharma, *Chem. Eng. J.*, 2022, **429**, 132384.
45 K. Manoli, G. Nakhla, A. K. Ray and V. K. Sharma, *Chem. Eng. J.*, 2017, **307**, 513–517.
46 S.-Q. Tian, L. Wang, Y.-L. Liu and J. Ma, *Water Res.*, 2020, **183**, 116054.
47 S. H. Wu, H. R. Li, X. Li, H. J. He and C. P. Yang, *Chem. Eng. J.*, 2018, **353**, 533–541.
48 V. K. Sharma, M. B. Feng, D. D. Dionysiou, H. C. Zhou, C. Jinadatha, K. Manoli, M. F. Smith, R. Luque, X. M. Ma and C. H. Huang, *Environ. Sci. Technol.*, 2022, **56**, 30–47.
49 V. K. Sharma, D. B. O'Connor and D. E. Cabelli, *J. Phys. Chem. B*, 2001, **105**, 11529–11532.
50 Y. Lee, R. Kissner and U. Von Gunten, *Environ. Sci. Technol.*, 2014, **48**, 5154–5162.
51 B. B. Shao, H. Y. Dong, B. Sun and X. H. Guan, *Environ. Sci. Technol.*, 2019, **53**, 894–902.
52 M. B. Feng and V. K. Sharma, *Chem. Eng. J.*, 2018, **341**, 137–145.
53 J. Zhang, L. Zhu, Z. Y. Shi and Y. Gao, *Chemosphere*, 2017, **186**, 576–579.
54 S. F. Sun, S. Y. Pang, J. Jiang, J. Ma, Z. S. Huang, J. M. Zhang, Y. L. Liu, C. B. Xu, Q. L. Liu and Y. X. Yuan, *Chem. Eng. J.*, 2018, **333**, 11–19.
55 A. Al-Abduly and V. K. Sharma, *J. Hazard. Mater.*, 2014, **279**, 296–301.
56 A. S. Kinsela, A. M. Jones, M. W. Bligh, A. N. Pham, R. N. Collins, J. J. Harrison, K. L. Wilsher, T. E. Payne and T. D. Waite, *Environ. Sci. Technol.*, 2016, **50**, 11663–11671.
57 G. E. Manger, *J. Sediment. Petrol.*, 1934, **4**, 141–151.
58 M. Esperanza, M. T. Suidan, F. Nishimura, Z.-M. Wang, G. A. Sorial, A. Zaffiro, P. McCauley, R. Brenner and G. Sayles, *Environ. Sci. Technol.*, 2004, **38**, 3028–3035.
59 H. M. Kuch and K. Ballschmiter, *Environ. Sci. Technol.*, 2001, **35**, 3201–3206.
60 G.-G. Ying, R. S. Kookana, A. Kumar and M. Mortimer, *Sci. Total Environ.*, 2009, **407**, 5147–5155.
61 W. Guan, Z. Xie and J. Zhang, *J. Spectrosc.*, 2014, **2014**, 1–8.
62 Z. Luo, M. Strouse, J.-Q. Jiang and V. K. Sharma, *J. Environ. Sci. Health, Part A: Environ. Sci. Eng.*, 2011, **46**, 453–460.
63 Y. Lee, J. Yoon and U. Von Gunten, *Water Res.*, 2005, **39**, 1946–1953.
64 Z. Wang, J. Jiang, S. Pang, Y. Zhou, C. Guan, Y. Gao, J. Li, Y. Yang, W. Qiu and C. Jiang, *Environ. Sci. Technol.*, 2018, **52**, 11276–11284.
65 L. Delaude and P. Laszlo, *J. Org. Chem.*, 1996, **61**, 6360–6370.
66 H. Kaur, S. Chaudhary, H. Kaur, M. Chaudhary and K. C. Jena, *ACS Appl. Nano Mater.*, 2022, **5**, 411–422.
67 S. Liu, Y. Sun, R. Wang, S. B. Mishra, H. Duan and H. Qu, *J. Cleaner Prod.*, 2020, **200**, 471–477.
68 I. Dayana, T. Sembiring, A. P. Tetuko, K. Sembiring, N. Maulida, Z. Cahyarani, E. A. Setiadi, N. S. Asri, M. Ginting and P. Sebayang, *J. Mol. Liq.*, 2019, **294**, 111557.
69 B. Y. Chen, H. W. Kuo, V. K. Sharma and W. Den, *Sci. Rep.*, 2019, **9**, 18268.
70 H. L. Wang, S. Q. Liu and X. Y. Zhang, *J. Hazard. Mater.*, 2009, **169**, 448–453.
71 B. L. Yuan, M. R. Ye and H. C. Lan, *Abstr. Pap. Am. Chem. Soc.*, 2006, **232**, 611.
72 X. F. Yan, J. Sun, A. Kenjiahan, X. H. Dai, B. J. Ni and Z. G. Yuan, *Water Res.*, 2020, **169**, 115208.
73 C. Li, X. Z. Li and N. Graham, *Chemosphere*, 2005, **61**, 537–543.

74 J. Yu, R. Jiao, H. Sun, H. Xu, Y. He and D. Wang, *J. Environ. Manage.*, 2022, **316**, 115328.
75 T. Kamachi, T. Kouno and K. Yoshizawa, *J. Org. Chem.*, 2005, **70**, 4380–4388.
76 Y. Jiang, J. E. Goodwill, J. E. Tobiason and D. A. Reckhow, *Environ. Sci. Technol.*, 2015, **49**, 2841–2848.
77 J. M. Schreyer and L. T. Ockerman, *Anal. Chem.*, 1951, **23**, 1312–1314.
78 M. M. Benjamin and D. F. Lawler, *Water Quality Engineering: Physical/Chemical Treatment Processes*, John Wiley & Sons, 2013.
79 X. Zhang, M. Feng, C. Luo, N. Nesnas, C.-H. Huang and V. K. Sharma, *Environ. Sci. Tehnol.*, 2021, **55**, 623–633.
80 J. E. Goodwill, Y. Jiang, D. A. Reckhow, J. Gikonyo and J. E. Tobiason, *Environ. Sci. Technol.*, 2015, **49**, 4955–4962.
81 Z.-S. Huang, L. Wang, Y.-L. Liu, J. Jiang, M. Xue, C.-B. Xu, Y.-F. Zhen, Y.-C. Wang and J. Ma, *Environ. Sci. Tehnol.*, 2018, **52**, 13897–13907.
82 M. Kolář, P. Novák, K. M. Šišková, L. Machala, O. Malina, J. Tuček, V. K. Sharma and R. Zbořil, *Phys. Chem. Chem. Phys.*, 2016, **18**, 4415–4422.
83 Y. Lee, J. Yoon and U. von Gunten, *Environ. Sci. Technol.*, 2005, **39**, 8978–8984.
84 H. Huang, D. Sommerfeld, B. C. Dunn, E. M. Eyring and C. R. Lloyd, *J. Phys. Chem. A*, 2001, **105**, 3536–3541.
85 J. Chen, Y. Qi, X. Pan, N. Wu, J. Zuo, C. Li, R. Qu, Z. Wang and Z. Chen, *Water Res.*, 2019, **158**, 338–349.
86 M. A. M. Rashid, M. Rahman, A. O. Mahmud, A. S. M. Morshed, M. M. Haque and M. M. Hossain, *Photochem*, 2022, **2**, 435–447.
87 Z. Moldovan, D. E. Popa, I. G. David, M. Buleandra and I. A. Badea, *J. Spectrosc.*, 2017, **2017**, 6929520.
88 J. Zhu, F. Yu, J. Meng, B. Shao, H. Dong, W. Chu, T. Cao, G. Wei, H. Wang and X. Guan, *Environ. Sci. Tehnol.*, 2020, **54**, 9702–9710.
89 S. F. Sun, J. Jiang, L. P. Qiu, S. Y. Pang, J. Li, C. H. Liu, L. H. Wang, M. Xue and J. Ma, *Water Res.*, 2019, **156**, 1–8.
90 M. Luo, H. Zhang, P. Zhou, Z. Xiong, B. Huang, J. Peng, R. Liu, W. Liu and B. Lai, *Water Res.*, 2022, **215**, 118243.
91 L. Pogliani, S. C. Ameta and A. K. Haghi, *Chemistry and Industrial Techniques for Chemical Engineers*, Apple Academic Press, Burlington ON; Palm Bay, Florida, 2021.
92 G. Wulfsberg, *Inorganic Chemistry*, University Science Books, Sausalito, Calif., 2000.